2012

Toward supramolecular architectures of the anti-HIV drug lamivudine: understanding the effect of the inclusion of water in a hydrochloride form

CRYSTENGCOMM, CAMBRIDGE, v. 14, n. 7, supl. 1, Part 3, pp. 2373-2376, NOV-DEC, 2012
http://www.producao.usp.br/handle/BDPI/42704

This article is published as part of the *CrystEngComm* themed issue entitled:

Crystal Engineering and Crystallography in the Pharmaceutical Industry

Guest Editors Magali Hickey, Örn Almarsson and Matt Peterson

Published in issue 7, 2012 of *CrystEngComm*

Articles in this issue include:

Highlight
The role of mechanochemistry and supramolecular design in the development of pharmaceutical materials
Amit Delori, Tomislav Friščić and William Jones

Highlight
Pharmaceutical crystallography: is there a devil in the details?
Andrew D. Bond

Paper
The effect of water molecules in stabilizing co-crystals of active pharmaceutical ingredients
Christer B. Aakeröy, Safiyyah Forbes and John Desper

CrystEngComm

Dynamic Article Links

Cite this: *CrystEngComm*, 2012, **14**, 2373

www.rsc.org/crystengcomm

COMMUNICATION

Toward supramolecular architectures of the anti-HIV drug lamivudine: understanding the effect of the inclusion of water in a hydrochloride form†

Javier Ellena,[b] Nikolas Paparidis[b] and Felipe Terra Martins*[ab]

Received 30th September 2011, Accepted 8th December 2011
DOI: 10.1039/c2ce06303d

Two salts of the anti-HIV drug lamivudine, namely, lamivudine hydrochloride and lamivudine hydrochloride monohydrate, were prepared for the first time. Structural relationships and the role of water in crystal assembly and lamivudine conformation were established and allowed for a rational approach to understand how solid state properties could be changed by engineering new salts of the drug.

The design of new smart crystalline phases of active pharmaceutical ingredients (API) and the understanding of structural relationships allow modulation of their solid state features related to the pharmaceutical performance.[1,2] Many drugs have very poor aqueous solubility and dissolution characteristics in their free base (or free acid) stable crystal forms, challenging researchers to solve this undesirable solid state feature. To improve APIs solubility, engineering and screening of salts, cocrystals, solvates, hydrates and polymorphs are commonly invoked.[3,4] In this sense, salt preparation of crystalline solids is one of the most attractive alternatives because of higher functional and technical characteristics of salts, such as solubility, stability and manufacturability, beyond low costs and practical procedures of preparation, high yield, reproducibility and purity.[5,6] Furthermore, the engineering, prediction and understanding of salt formation are based on elegant chemical approaches on assembly mechanisms driven by molecular recognition events, which contribute to an easier legal process for protection of intellectual property on novel API crystal phases due to nonobviousness of designed molecular salts.[7]

Lamivudine (β-L-2′,3′-dideoxy-3′-thiacytidine, 3TC) belongs to the class of nucleoside reverse transcriptase inhibitors (NRTIs), and it is being used worldwide in anti-HIV therapy[8] and also against hepatitis B virus.[9] Lamivudine can be described as a cytidine analog having a sulfur atom at 3′-position instead of methylene group as occurs in the canonical nucleoside. Concerning its asymmetry centers, the two chiral C1′ and C4′ carbons are present with *S* and *R* absolute configurations, respectively. Due to this chirality, lamivudine always crystallizes in non-centrosymmetric space groups. Recent studies have demonstrated the ability of lamivudine to crystallize together with several small molecules in multicomponent molecular co-crystals,[10–13] even though simple salts of the drug with inorganic counterions have not been reported.

Indeed, APIs containing protonable imine groups such as lamivudine can form salts with simple inorganic acids such as hydrochloric acid. Here, we reported the preparation‡ and the crystal structures§ of two lamivudine salts, namely, lamivudine hydrochloride (**1**) and lamivudine hydrochloride monohydrate (**2**).

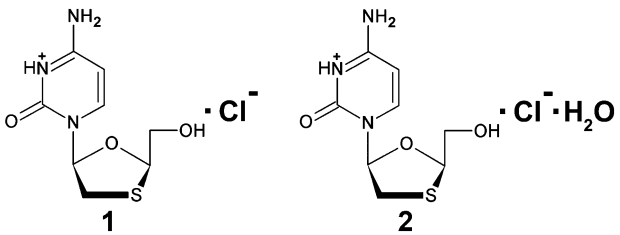

Lamivudine stoichiometrically crystallized together with hydrochloric acid in two salt forms depending on the solvent system. An anhydrate phase and a monohydrate form of lamivudine hydrochloride were synthesized after solvent combinations and hydrochloric acid concentrations in water solutions were screened. From the three-component system of lamivudine, 0.28 mol L^{-1} solution of hydrochloric acid in water and isopropanol, crystals of **1** were obtained, while crystals of **2** were isolated from the two-component system of lamivudine and the same water solution of hydrochloric acid. According to the hydrochloric acid concentrations used in both crystallization media, the pH values of the two solvent systems were below 2. Under such acidic conditions, the conjugated acid form of lamivudine (pK_a 4.30)[14] prevailed over the neutral one. Before the solvent system began to evaporate, the concentration of the protonated form already was at least 200-fold higher than that of the base. By using both crystallization systems described above, it was expected therefore that lamivudine would assemble into solid state phases only made up of positively charged drug molecules, as it was observed in the structures of **1** and **2**.

Both lamivudine salts crystallize in the $P2_1$ space group with one $(lamivudine)^+$ cation and one chloride anion in the asymmetric units (Fig. 1). One water molecule also composes the asymmetric unit of the salt hydrate. In **1** and **2**, the drug backbones resemble one another

[a]*Instituto de Química, Universidade Federal de Goiás, Campus Samambaia, CP 131, 74001-970 Goiânia, GO, Brazil. E-mail: felipe@quimica.ufg.br; Fax: +55 62 3521 1167; Tel: +55 62 3521 1097*
[b]*Instituto de Física de São Carlos, Universidade de São Paulo, CP 369, 13560-970 São Carlos, SP, Brazil*

† CCDC reference numbers 751365–751368. For crystallographic data in CIF or other electronic format see DOI: 10.1039/c2ce06303d

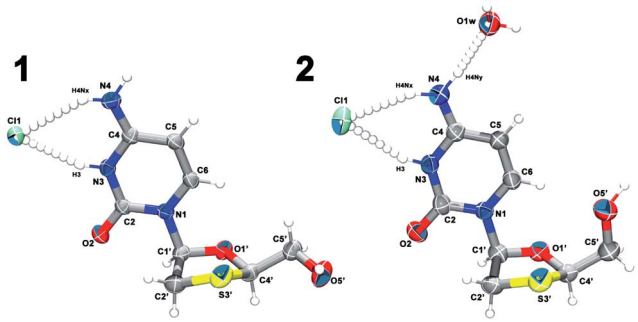

Fig. 1 Asymmetric units of lamivudine hydrochloride (**1**) and lamivudine hydrochloride monohydrate (**2**). Hydrogens are outlined as arbitrary radius spheres, and the ellipsoids are at the 50% probability level.

and both exhibit a conformation commonly found in canonical nucleotides of DNA (Fig. 2). Cytosine and oxathiolane rings are present with an *anti* conformation (C2–N1–C1′–O1′ torsion measures 161.9(2)°[15] and 164.2(3)° in **1** and **2**) and C3′-*endo* pucker (C2′–C1′–O1′–C4′ torsion measures −7.1(3)° and −10.2(4)° in **1** and **2**), respectively.

However, there is a great conformational difference between the drug backbones. In the salt anhydrate, the hydroxyl group bonded to the methylene sp^3-hybridized 5′-carbon adopts an equatorial position on the same side of the sulfur atom of the five-membered oxathiolane ring. In contrast, the 5′-hydroxyl group is axially bonded to carbon on the same side of cytosine in **2**, in an equivalent position of one of the two 5′-methylene hydrogens of **1** (Fig. 2). These conformations observed in lamivudine molecules of the hydrochloride salts are related to a rotation of about 120° on the C4′–C5′ bond axis. It is important to highlight that the CH_2OH group conformations are related to the hydrogen bonding patterns assembling the hydrochloride salt structures (see in sequence). The O1′–C4′–C5′–O5′ and S3′–C4′–C5′–O5′ dihedral angles measure −175.8(2)° and 65.1(3)° in **1** and 63.4(4)° and −57.4(4)° in **2**. One can observe that there are gaps of 239.2° and 122.5° in the values of the O1′–C4′–C5′–O5′ and S3′–C4′–C5′–O5′ torsions between the hydrochloride salts of lamivudine, which is in agreement with the 3-fold rotation on the C4′–C5′ bond axis.

Supramolecular architectures of **1** and **2** were layered with lamivudine molecules base-stacked along the [100] direction through π–π interactions, with interlayer spaces measuring 3.28(4) Å and 3.30(1) Å, respectively. Furthermore, each chloride anion is a double

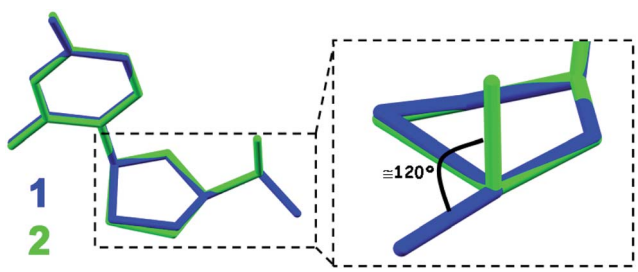

Fig. 2 Superposition of lamivudine conformers assembling the structures of **1** and **2**. The hydrogen atoms were hidden for clarity. Oxathiolane rings are highlighted in order to detach the 3-fold rotation on the C4′–C5′ bond axis.

hydrogen bonding acceptor from lamivudine in both structures. Through their imine and amine groups, protonated cytosine rings of the drug donate hydrogen bonds to chloride in a bifurcated pattern (Fig. 3). In **1**, the other NH_2 hydrogen that is not involved in the bifurcated hydrogen bonds also interacts with a 2_1-screw axis symmetry related chloride anion, which assembles one-dimensional chains parallel to the [010] direction made up of alternate cations and anions. Along this direction, lamivudine units related by the 2_1-screw axis symmetry are connected through a classical hydrogen bonding between the 5′-hydroxyl and 2-carbonyl groups. This O–H···O contact can be viewed as a cross-linker between the [010]-packed chains of **1** along the [10$\bar{1}$] direction, giving rise to hydrogen bonded 2D layers (Fig. 3). In **2**, the other NH_2 hydrogen is hydrogen bonded to water that lies in the position of a 2_1-screw axis symmetry related chloride which would be connected to the amine hydrogen in **1**. In this way, in the salt hydrate water plays the hydrogen bonding acceptor role of a chloride in **1**. Furthermore, each water molecule is a double hydrogen bonding donor to chloride anions. This hydrogen bonding pattern gives rise to wires of alternate chloride and water fragments along the [100] direction in which lamivudine molecules are anchored by means of hydrogen bonding donation through their cytosine fragments (Fig. 3). In addition, the hydrogen bonding between the 5′-hydroxyl and 2-carbonyl groups also occurs in **2**, although lamivudine molecules hydrogen bonded through this contact are related by the translation symmetry in this structure. The wires made up of water and chloride anions with attached lamivudine cations are 2_1-screw axis symmetry related in **2**. These supramolecular wires are packed along the *b* axis only through vdW interactions.

By inspecting both structures of **1** and **2**, conformational differences and crystal assembly changes can be understood as consequences of water inclusion (Fig. 4). Water is a hydrogen bonding acceptor from lamivudine and also acts as a "molecular hook"[16] to connect translation symmetry related $(lamivudine)^+(Cl)^-$ pairs along the [101] direction in **2**. The "water hook" donates one of the two hydrogens to a chloride of an adjacent $(lamivudine)^+(Cl)^-$ pair arranged parallel to this crystallographic direction. This interaction between water and chloride is related to the conformational difference aforementioned. The presence of water molecules in the lattice as hydrogen bonding donors to chloride anions becomes close together translation symmetry related lamivudine molecules so that the O–H···O hydrogen bonding between them is formed. Relative to the salt anhydrate, a 3-fold rotation on the C4′–C5′ bond axis occurs in the salt hydrate to position the 5′-hydroxyl group of one lamivudine molecule toward the carbonyl moiety of another one (Fig. 4).

In an attempt to predict solid state properties related to the pharmaceutical performance of these new lamivudine salts, relationships between structural features and crystal packing efficiency were established. As it was before described, classical hydrogen bonds between lamivudine molecules and chloride counterions and between lamivudine molecules are responsible for the assembly of strongly bonded 2D layers that are stacked on top of each other to form a closely packed 3D network in **1**, while only weak contacts pack lamivudine-anchored chloride-water wires along the [010] direction of **2**. Consequently, we can conclude that the crystal packing of **1** is more efficient than that of **2**, which is corroborated by the fact that the calculated density of **1** (1.599 g cm^{-3}) is higher than that of **2** (1.524 g cm^{-3}). This approach can be useful to rationalize solid state behaviors of the salts, as, for instance, equilibrium solubility and kinetic dissolution.

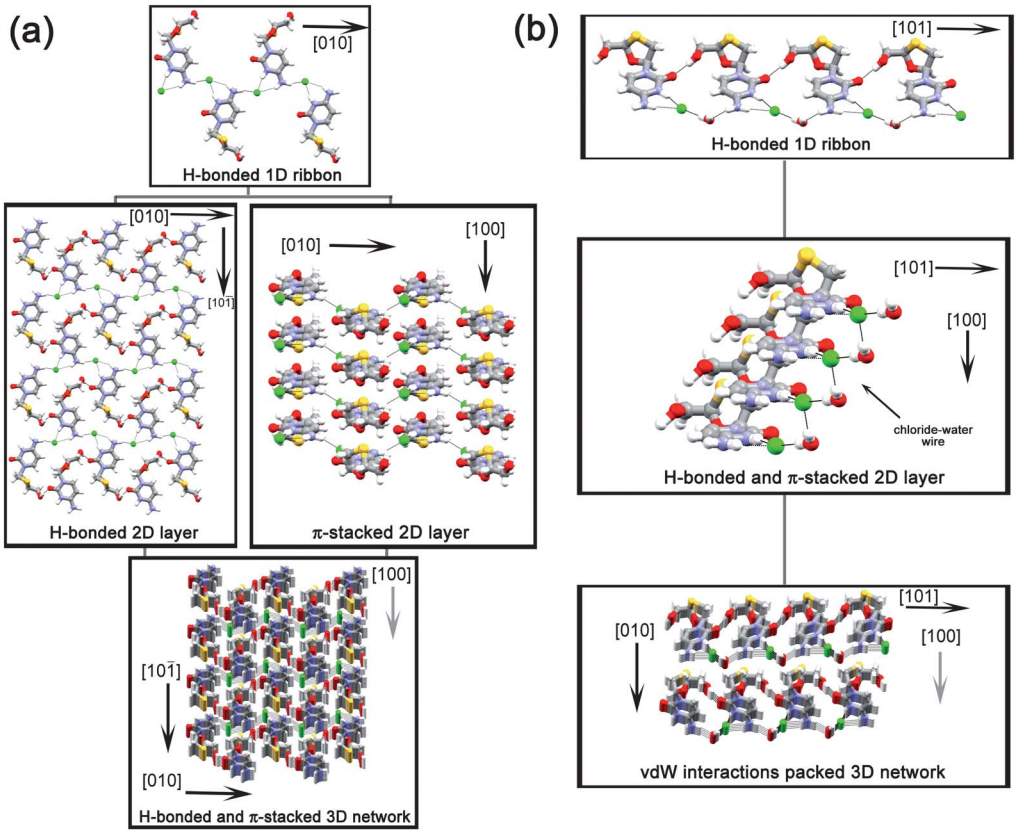

Fig. 3 Assembling the structures of (a) **1** and (b) **2**. Black and gray arrows indicate the crystallographic directions parallel and normal to the projection planes, respectively.

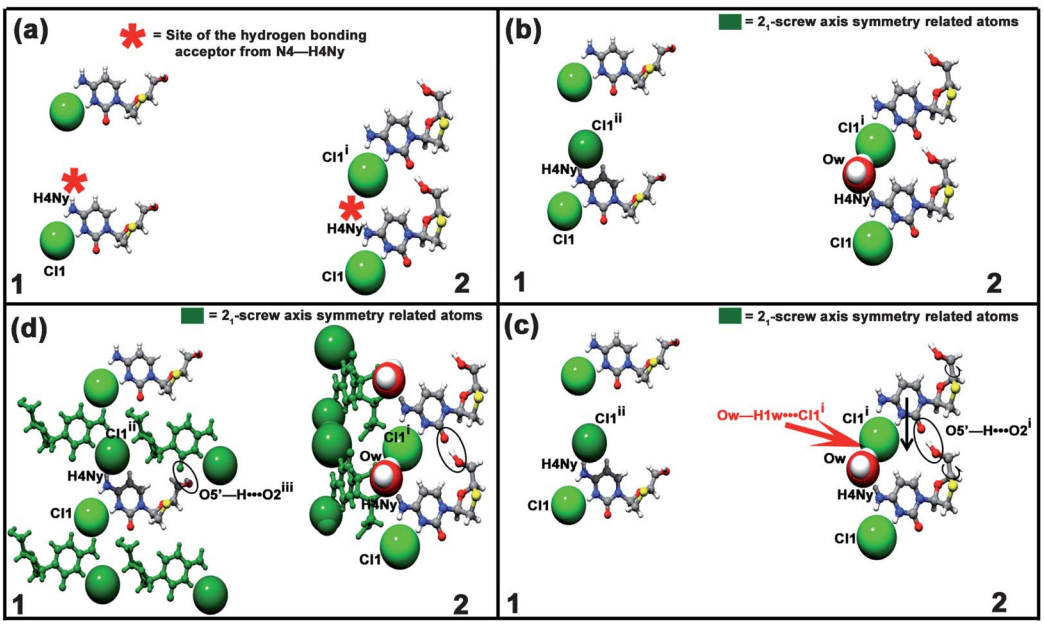

Fig. 4 Effect of the water inclusion in the crystal lattice of **2**. (a) Two translation symmetry related (lamivudine)$^{+}$Cl^{-} pairs are packed along the [010] and [101] directions in **1** and **2**, respectively. (b) In **2**, water lies in the corresponding site of a 2_1-screw axis symmetry related chloride anion of **1**. (c) The hydrogen bonding between water and a translation symmetry related chloride anion (red arrow) is responsible for the displacement of a neighboring (lamivudine)$^{+}$Cl^{-} pair (black arrow) and then driving the rotation on the C4′–C5′ bond axis to form the hydrogen bonding between the 5′-hydroxyl and 2-carbonyl groups (circled) of translation symmetry related molecules. (d) In **1**, the hydrogen bonding between the 5′-hydroxyl and 2-carbonyl groups occurs between 2_1-screw axis symmetry related lamivudine fragments. Equivalent positions: (i) $1 + x, y, 1 + z$; (ii) $-x, -0.5 + y, 1 - z$; (iii) $1 - x, -0.5 + y, -z$.

In summary, anhydrate and monohydrate versions of lamivudine hydrochloride were prepared and their structures were elucidated and understood on the basis of crystal assembly inspections and conformational analyses. Such structural knowledge will be of valuable use for the comprehension of related solid state features. Because most hydrochloride salts are more soluble than the parent APIs, these new lamivudine salts reported here are expected to be improved from a pharmaceutical point of view, meaning an important advance in the solid state chemistry of lamivudine.

Acknowledgements

We thank the Brazilian Research Council CNPq (Conselho Nacional de Desenvolvimento Científico e Tecnológico) for the financial support (Processo 472623/2011-7 - Universal 14/2011). Thanks are due to the Consejo Superior de Investigaciones Científicas (CSIC) of Spain for the award of a license for the use of the Cambridge Structural Database (CSD).

Notes and references

‡ *Preparation*. Lamivudine form II was used as the starting material for preparation of **1** and **2**. The authenticity and purity of lamivudine form II were first confirmed by single crystal and powder X-ray diffraction techniques before using it to prepare the crystalline modifications. For preparation of **1**, a quantity of the drug (10 mg, 0.04 mmol) was dissolved in isopropanol (5 ml, 66 mmol) under stirring (5 min) on a water bath (308 K). The solution was then allowed to cool to room temperature. By adding a 0.28 mol L^{-1} solution of hydrochloric acid in water (0.25 ml, 0.07 mmol) to the preparation of the drug in isopropyl alcohol, crystals of **1** could be obtained after stirring (5 min, 298 K) and slow evaporation of the resulting solution upon standing (7 days, 298 K). On the other hand, by dissolution of lamivudine (10 mg, 0.04 mmol) in double-distilled water (5 ml, 0.28 mol) under shaking (10 min) on a water bath (313 K), crystals of **2** were obtained after addition of the same hydrochloric acid solution (0.25 ml, 0.07 mmol) to the aqueous solution of lamivudine, cooling to room temperature, stirring of the mixture (5 min, 298 K) and standing for 8 days at room temperature.

§ *Structure determination*. Well-grown single crystals of **1** and **2** measuring 0.43 × 0.10 × 0.05 mm^3 and 0.58 × 0.10 × 0.03 mm^3, respectively, were isolated from the glass crystallizers after the crystallization period. They were mounted on a κ-goniostat and exposed to graphite-monochromated X-ray beam (Mo Kα, $\lambda = 0.71073$ Å) using an Enraf-Nonius Kappa-CCD diffractometer equipped with a CCD camera of 95 mm. The data collection strategy was calculated by setting φ scans and ω scans with κ offsets. The crystallographic software used was as follows: COLLECT[17] (X-ray diffraction experiment monitoring), HKL Denzo–Scalepack[18] package of software (indexing, integration and scaling of raw data), SHELXS-97 (ref. 19) (structure solving), SHELXL-97 (ref. 19) (structure refinement), MERCURY[20] and ORTEP-3 (ref. 21) (structure analysis and graphical representations). The structures were solved using the direct methods of phase retrieval, in which all non-hydrogen atoms of an asymmetric unit were located from the electronic density Fourier map. The solved model was refined by the full-matrix least squares method based on F^2. In the refinements, free anisotropic and fixed isotropic thermal displacement parameters were set for non-hydrogen and hydrogen atoms, respectively. The isotropic thermal displacement parameters of the C–H and N–H hydrogen atoms were 20% greater than the equivalent isotropic parameter of the corresponding atom. For the O–H hydrogen atoms, this percentage was set to 50%. Concerning the positions of hydrogens, C–H bond distances were stereochemically defined according to the riding model. Therefore, (x, y, z) fractional coordinates of these hydrogen atoms were constrained in the refinements. The coordinates of O–H, N–H and N^+–H hydrogen atoms were primarily defined as those of the electronic density peaks located from the difference Fourier map. After these positions were taken, they were refined freely.

Crystal data for **1**. $(C_8H_{12}N_3O_3S)Cl$, $M_w = 265.72$, monoclinic, $a = 5.7060(2)$ Å, $b = 11.9670(5)$ Å, $c = 8.3401(4)$ Å, $\beta = 104.273(2)^\circ$, $V = 551.91(4)$ $Å^3$, $T = 298(2)$ K, space group $P2_1$, $Z = 2$, $D_c = 1.599$ g cm^{-3}, μ(MoKα) = 0.531 mm^{-1}, GAUSSIAN absorption correction ($T_{min} = 0.866$, $T_{max} = 0.974$), θ-range for data collection = 3.04–26.63, $-6 \le h \le 7$, $-14 \le k \le 15$, $-10 \le l \le 10$, 6374 reflections collected, 2284 unique ($R_{int} = 0.0646$), completeness to $\theta = 26.63$ of 99.0%, $F_{000} = 276$, 157 parameters refined, $S = 1.030$, $R_1(I > 2\sigma(I)) = 0.0365$, $wR_2(I > 2\sigma(I)) = 0.0896$, R_1(all data) = 0.0438, wR_2(all data) = 0.0943, largest diff. peak/hole = 0.293/−0.234 e $Å^{-3}$, Flack parameter = 0.09(7) (1080 Friedel pairs), CCDC-751365 (for low temperature structure, CCDC-751367).

Crystal data for **2**. $(C_8H_{12}N_3O_3S)(H_2O)Cl$, $M_w = 283.73$, monoclinic, $a = 5.2927(2)$ Å, $b = 17.252(1)$ Å, $c = 6.8518(4)$ Å, $\beta = 98.865(3)^\circ$, $V = 618.18(6)$ $Å^3$, $T = 298(1)$ K, space group $P2_1$, $Z = 2$, $D_c = 1.524$ g cm^{-3}, μ(MoKα) = 0.485 mm^{-1}, GAUSSIAN absorption correction ($T_{min} = 0.881$, $T_{max} = 0.986$), θ-range for data collection = 3.83–25.10, $-6 \le h \le 5$, $-19 \le k \le 19$, $-7 \le l \le 7$, 7849 reflections collected, 1854 unique ($R_{int} = 0.0840$), completeness to $\theta = 25.10$ of 98.9%, $F_{000} = 296$, 172 parameters refined, $S = 1.039$, $R_1(I > 2\sigma(I)) = 0.0364$, $wR_2(I > 2\sigma(I)) = 0.0754$, R_1(all data) = 0.0528, wR_2(all data) = 0.0823, largest diff. peak/hole = 0.164/−0.212 e $Å^{-3}$, Flack parameter = −0.06(8) (889 Friedel pairs), CCDC-751366 (for low temperature structure, CCDC-751368).

1 L. F. Huang and W. Q. Tong, *Adv. Drug Delivery Rev.*, 2004, **56**, 321.
2 D. Singhal and W. Curatolo, *Adv. Drug Delivery Rev.*, 2004, **56**, 335.
3 P. Vishweshwar, J. A. Mcmahon, M. L. Peterson, M. B. Hickey, T. R. Shattock and M. J. Zaworotko, *Chem. Commun.*, 2005, 4601.
4 C. B. Aakeroy, M. E. Fasulo and J. Desper, *Mol. Pharmaceutics*, 2007, **4**, 317.
5 F. Lara-Ochoa and G. Espinosa-Pérez, *Cryst. Growth Des.*, 2007, **7**, 1213.
6 Ö. Almarsson and M. J. Zaworotko, *Chem. Commun.*, 2004, 1889.
7 A. V. Trask, *Mol. Pharmaceutics*, 2007, **4**, 301.
8 J. A. V. Coates, N. Cammack, H. J. Jenkinson, I. M. Mutton, B. A. Pearson, R. Storer, J. M. Cameron and C. R. Penn, *Antimicrob. Agents Chemother.*, 1992, **36**, 202.
9 C. N. Chang, V. Skalskiv, J. H. Zhou and Y. C. Cheng, *J. Biol. Chem.*, 1992, **267**, 22414.
10 R. Banerjee, P. M. Bhatt, N. V. Ravindra and G. R. Desiraju, *Cryst. Growth Des.*, 2005, **5**, 2299.
11 P. M. Bhatt, Y. Azim, T. S. Thakur and G. R. Desiraju, *Cryst. Growth Des.*, 2009, **9**, 951.
12 F. T. Martins, N. Paparidis, A. C. Doriguetto and J. Ellena, *Cryst. Growth Des.*, 2009, **9**, 5283.
13 F. T. Martins, A. C. Doriguetto and J. Ellena, *Cryst. Growth Des.*, 2010, **10**, 676.
14 M. Shalaeva, J. Kenseth, F. Lombardo and A. Bastinz, *J. Pharm. Sci.*, 2008, **97**, 2581.
15 X-Ray diffraction experiments were carried out both at room and low temperatures. The crystals were frozen by using a cold N_2 gas blower cryogenic device (Oxford Cryosystem, Oxford) when collecting X-ray diffraction intensities at low temperature. These analyses revealed that no solid–solid phase transformation between the evaluated temperatures occurs in all structures. This is concluded because there are only slight variations in the unit cell parameters and the crystal structures are similar under different temperatures. All figures were prepared using room temperature structures. Likewise, geometrical parameters presented throughout the text were inspected from the structures determined using X-ray diffraction data collected at room temperature.
16 S. Varughese and G. R. Desiraju, *Cryst. Growth Des.*, 2010, **10**, 4184.
17 COLLECT, *Data Collection Software*, Nonius, Delft, The Netherlands, 1998.
18 Z. Otwinowski and W. Minor, in *Methods in Enzymology: Macromolecular Crystallography, Part A*, ed. C. W. Carter, Jr and R. M. Sweet, Academic Press, New York, 1997, vol. 276, pp. 307–326.
19 G. M. Sheldrick, *Acta Crystallogr., Sect. A: Found. Crystallogr.*, 2008, **64**, 112.
20 C. F. Macrae, I. J. Bruno, J. A. Chisholm, P. R. Edgington, P. Mccabe, E. Pidcock, L. R. Monge, R. Taylor, J. van de Streek and P. A. Wood, *J. Appl. Crystallogr.*, 2008, **41**, 466.
21 L. J. Farrugia, *J. Appl. Crystallogr.*, 1997, **30**, 565.

